Soft x-ray free electron laser microfocus for exploring matter under extreme conditions

A. J. Nelson*[1], S. Toleikis[2], H. Chapman[2], S. Bajt[3], J. Krzywinski[4], J. Chalupsky[5,6], L. Juha[5], J. Cihelka[5,7], V. Hajkova[5], L. Vysin[5,6], T. Burian[5,6], M. Kozlova[5], R.R. Fäustlin[3], B. Nagler[8], S.M. Vinko[8], T. Whitcher[8], T. Dzelzainis[9], O. Renner[5], K. Saksl[10], A. R. Khorsand[11], P. A. Heimann[12], R. Sobierajski[13], D. Klinger[13], M. Jurek[13], J. Pelka[13], B. Iwan[14], J. Andreasson[14], N. Timneanu[14], M. Fajardo[15], J.S. Wark[8], D. Riley[9], T. Tschentscher[3], J. Hajdu[14], R. W. Lee[1]

[1]LawrenceLivermore National Laboratory, 7000 East Avenue, Livermore, CA 94550, USA
[2]CFEL/University of Hamburg, Notkestraße 85, D-22607 Hamburg, Germany
[3]Deutsches Elektronen-Synchrotron DESY, Notkestrasse 85, D-22607 Hamburg, Germany
[4]SLAC National Accelerator Laboratory, 2575 Sand Hill Road, Menlo Park, CA 94025, USA
[5]Institute of Physics ASCR, Na Slovance 2, 182 21 Prague 8, Czech Republic
[6]Czech Technical University in Prague, Zikova 1905/4, 166 36 Praha 6, Czech Republic
[7]J. Heyrovský Institute of Physical Chemistry ASCR, Dolejškova 3,182 23 Prague 8, Czech Republic
[8]Department of Physics, Clarendon Laboratory, University of Oxford, Parks Road, Oxford, OX1 3PU, UK
[9]Queen's University Belfast, University Road Belfast, BT7 1NN, Northern Ireland, UK
[10]Institute of Materials Research SAS, Watsonova 47, 040 01 Kosice, Slovak Republic
[11]FOM-Institute for Plasma Physics Rijnhuizen, P.O. Box 1207, 3430 BE Nieuwegein, The Netherlands
[12]Lawrence Berkeley National Laboratory, 1 Cyclotron Road, CA 94720, USA
[13]Institute of Physics PAS, Al. Lotników 32/46, PL-02-668 Warsaw, Poland
[14]Molecular Biophysics, Uppsala University, Husargatan 3, Box 596, SE-75124, Uppsala, Sweden
[15]Centro de Fsica dos Plasmas, Instituto Superior Tecnico, Lisboa, Portugal
**nelson63@llnl.gov*

Abstract: We have focused a beam (BL3) of FLASH (Free-electron LASer in Hamburg: λ = 13.5 nm, pulse length 15 fs, pulse energy 10-40 μJ, 5Hz) using a fine polished off-axis parabola having a focal length of 270 mm and coated with a Mo/Si multilayer with an initial reflectivity of 67% at 13.5 nm. The OAP was mounted and aligned with a picomotor controlled six-axis gimbal. Beam imprints on poly(methyl methacrylate) - PMMA were used to measure focus and the focused beam was used to create isochoric heating of various slab targets. Results show the focal spot has a diameter of ≤1μm. Observations were correlated with simulations of best focus to provide further relevant information.

OCIS codes: (140.2600) Free-electron lasers (FELs); (340.7480) X-rays, soft x-rays, extreme ultraviolet (EUV).

References and links

1. W. Ackermann, G. Asova, V. Ayvazyan, A. Azima, N. Baboi, J. Bähr, V. Balandin, B. Beutner, A. Brandt, A. Bolzmann, R. Brinkmann, O. I. Brovko, M. Castellano, P. Castro, L. Catani, E. Chiadroni, S. Choroba, A. Cianchi, J. T. Costello, D. Cubaynes, J. Dardis, W. Decking, H. Delsim-Hashemi, A. Delserieys, G. Di Pirro, M. Dohlus, S. Düsterer, A. Eckhardt, H. T. Edwards, B. Faatz, J. Feldhaus, K. Flöttmann, J. Frisch, L. Fröhlich, T. Garvey, U. Gensch, C. Gerth, M. Görler, N. Golubeva, H.-J. Grabosch, M. Grecki, O. Grimm, K. Hacker, U. Hahn, J. H. Han, K. Honkavaara, T. Hott, M. Hüning, Y. Ivanisenko, E. Jaeschke, W. Jalmuzna, T. Jezynski, R. Kammering, V. Katalev, K. Kavanagh, E. T. Kennedy, S. Khodyachykh, K. Klose, V. Kocharyan, M. Körfer, M. Kollewe, W. Koprek, S. Korepanov, D. Kostin, M. Krassilnikov, G. Kube, M. Kuhlmann, C. L. S. Lewis, L. Lilje, T. Limberg, D. Lipka, F. Löhl, H. Luna, M. Luong, M. Martins, M. Meyer, P. Michelato, V. Miltchev, W. D. Möller, L. Monaco, W. F. O. Müller, O. Napieralski, O. Napoly, P. Nicolosi, D. Nölle, T. Nuñez, A. Oppelt, C. Pagani, R. Paparella, N. Pchalek, J. Pedregosa-Gutierrez, B. Petersen, B. Petrosyan, G. Petrosyan, L. Petrosyan, J. Pflüger, E. Plönjes, L. Poletto, K. Pozniak, E. Prat, D. Proch, P. Pucyk, P. Radcliffe, H. Redlin, K. Rehlich, M. Richter, M. Roehrs, J. Roensch, R. Romaniuk, M. Ross, J. Rossbach, V. Rybnikov, M. Sachwitz, E. L. Saldin, W. Sandner, H. Schlarb, B. Schmidt, M. Schmitz, P. Schmüser, J. R. Schneider, E. A. Schneidmiller, S. Schnepp, S. Schreiber, M. Seidel, D. Sertore, A. V. Shabunov, C. Simon, S. Simrock, E. Sombrowski, A. A. Sorokin, P. Spanknebel, R. Spesyvtsev, L. Staykov, B. Steffen, F. Stephan, F. Stulle, H. Thom, K. Tiedtke, M. Tischer, S. Toleikis, R. Treusch, D. Trines, I. Tsakov, E. Vogel, T. Weiland, H. Weise, M. Wellhöfer, M. Wendt,

#114017 - $15.00 USD Received 8 Jul 2009; revised 14 Aug 2009; accepted 1 Sep 2009; published 25 Sep 2009

I. Will, A. Winter, K. Wittenburg, W. Wurth, P. Yeates, M. V. Yurkov, I. Zagorodnov, and K. Zapfe, "Operation of a free-electron laser from the extreme ultraviolet to the water window," Nat. Photonics **1**(6), 336–342 (2007).
2. J. Chalupský, L. Juha, V. Hájková, J. Cihelka, L. Vysín, J. Gautier, J. Hajdu, S. P. Hau-Riege, M. Jurek, J. Krzywinski, R. A. London, E. Papalazarou, J. B. Pelka, G. Rey, S. Sebban, R. Sobierajski, N. Stojanovic, K. Tiedtke, S. Toleikis, T. Tschentscher, C. Valentin, H. Wabnitz, and P. Zeitoun, "Non-thermal desorption/ablation of molecular solids induced by ultra-short soft x-ray pulses," Opt. Express **17**(1), 208–217 (2009).
3. B. Nagler, U. Zastrau, R. Fäustlin, S. M. Vinko, T. Whitcher, A. J. Nelson, R. Sobierajski, J. Chalupsky, E. Abreu, S. Bajt, T. Bornath, T. Burian, H. Chapman, J. Cihelka, T. Döppner, S. Düsterer, T. Dzelzainis, M. Fajardo, E. Förster, C. Fortmann, E. J. Galtier, S. H. Glenzer, S. Göde, G. Gregori, V. Hajkova, P. Heimann, L. Juha, M. Jurek, F. Y. Khattak, A. R. Khorsand, D. Klinger, M. Kozlova, J. Krzywinski, T. Laarmann, H. J. Lee, R. Lee, K.-H. Meiwes-Broer, P. Mercere, W. J. Murphy, A. Przystawik, R. Redmer, H. Reinholz, D. Riley, G. Röpke, F. Rosmej, K. Saksl, R. Schott, R. Thiele, J. Tiggesbäumker, S. Toleikis, T. Tschentscher, I. Uschmann, H. J. Vollmer, and J. Wark, "Transparency induced in solid density aluminum by ultra-intense XUV radiation," Nat. Phys. **5**, 1341 (2009).
4. J. Bauer, L. Plucinski, B. Piraux, R. Potvliege, M. Gajda, and J. Krzywinski,Ionization of hydrogen atoms by intense vacuum ultraviolet radiation," J. Phys. B **34**(11), 2245–2254 (2001).
5. A. Maréchal, "Etudes des effets combinés de la diffraction et des aberrations géometrique sur l'image d'un point lumineux," Rev. Opt. Theor. Instrum. **26**, 257–277 (1947).
6. J. C. Wyant, and K. Creath, *Basic Wavefront Aberration Theory for Optical Metrology*, Applied Optics and Optical Engineering, Volume XI, (Academic Press, San Diego, 1992) pp. 38–39.
7. S. Bajt, H. Chapman, A. J. Nelson, R. W. Lee, S. Toleikis, P. Mirkarimi, J. Alameda, S. Baker, H. Vollmer, R. Graff, A. Aquila, E. Gullikson, J. Meyer Ilse, E. Spiller, J. Krzywinski, L. Juha, J. Chalupský, V. Hájková, J. Hajdu, and T. Tschentscher, "Sub-micron focusing of a soft X-ray Free Electron Laser beam", Proc. of SPIE Vol. 7361, 73610J1–10 (2009).
8. J. H. Underwood, and E. M. Gullikson, "High-resolution, high-flux, user friendly VLS beamline at the ALS for the 50–1300 eV energy region," J. Electron Spectrosc. Relat. Phenom. **92**(1-3), 265–272 (1998).
9. J. W. Goodman, "Introduction to Fourier Optics", Mc Graw-Hill, 1968.
10. J. Krzywinski, unpublished.
11. L. Juha, M. Bittnera, D. Chvostova, V. Letal, J. Krasa, Z. Otcenasek, M. Kozlova, J. Polan, A. R. Präg, B. Rus, M. Stupka, J. Krzywinski, A. Andrejczuk, J. B. Pelka, R. Sobierajski, L. Ryc, J. Feldhaus, F. P. Boody, M. E. Grisham, G. O. Vaschenko, C. S. Menoni, and J. J. Rocca, "XUV-laser induced ablation of PMMA with nano-, pico-, and femtosecond pulses," J. Electron Spectrosc. Relat. Phenom. **144–147**, 929–932 (2005).
12. J. Chalupský, L. Juha, J. Kuba, J. Cihelka, V. Hájková, S. Koptyaev, J. Krása, A. Velyhan, M. Bergh, C. Caleman, J. Hajdu, R. M. Bionta, H. Chapman, S. P. Hau-Riege, R. A. London, M. Jurek, J. Krzywinski, R. Nietubyc, J. B. Pelka, R. Sobierajski, J. Meyer-Ter-Vehn, A. Tronnier, K. Sokolowski-Tinten, N. Stojanovic, K. Tiedtke, S. Toleikis, T. Tschentscher, H. Wabnitz, and U. Zastrau, "Characteristics of focused soft X-ray free-electron laser beam determined by ablation of organic molecular solids," Opt. Express **15**(10), 6036–6043 (2007).
13. B. R. Benware, A. Ozols, J. J. Rocca, I. A. Artioukov, V. V. Kondratenko, and A. V. Vinogradov, "Focusing of a tabletop soft-x-ray laser beam and laser ablation," Opt. Lett. **24**(23), 1714–1716 (1999).
14. S. Kazamias, K. Cassou, O. Guilbaud, A. Klisnick, D. Ros, F. Ple, G. Jamelot, B. Rus, M. Koslova, M. Stupka, T. Mocek, D. Douillet, P. Zeitoun, D. Joyeux, and D. Phalippou, "Homogeneous focusing with a transient soft X-ray laser for irradiation experiments," Opt. Commun. **263**(1), 98–104 (2006).
15. T. Mocek, B. Rus, M. Stupka, M. Kozlová, A. R. Präg, J. Polan, M. Bittner, R. Sobierajski, and L. Juha,Focusing a multimillijoule soft x-ray laser at 21 nm," Appl. Phys. Lett. **89**(5), 051501 (2006).
16. M. Berrill, F. Brizuela, B. Langdon, H. Bravo, C. S. Menoni, and J. J. Rocca, "Photoionized plasmas created by soft-x-ray laser irradiation of solid targets," J. Opt. Soc. Am. B **25**(7), B32–B38 (2008).

1. Introduction

The properties of 4th-generation Free Electron Laser (FEL) sources are revolutionizing the field of fast time-resolved x-ray science with the realization of sub-ps material response due to the ultrashort pulses and high intensity coherent monochromatic radiation. The free-electron laser in Hamburg (FLASH) [1] in routine operation produces soft X-ray pulses at several wavelengths (32.5, 13.5, 7 nm) yielding 10^{14} W/cm^2 at a 20 μm focus. This 4th-generation light source has allowed advanced studies of high-intensity laser-matter interactions on the femtosecond time scale [2,3].

Tightly focused FEL beams are necessary for high intensity irradiation of samples to perform warm dense matter studies, single molecule X-ray diffraction imaging and various pump probe experiments since the samples are very small with weak scattering centers. Submicron focus will permit us to reach intensities $\geq 10^{17}$ W/cm^2 that in turn would allow us to enter the non-perturbative regime in atomic physics in the soft X-ray range [4].

To reach the high intensities unique to 4th generation light sources, and unattainable by current synchrotrons, challenging substrate requirements for normal incidence focusing optics

#114017 - $15.00 USD Received 8 Jul 2009; revised 14 Aug 2009; accepted 1 Sep 2009; published 25 Sep 2009

need to be met. For example, Fig. 1 shows the necessary surface figure for optic substrates used in a normal incidence geometry that is needed to reach the Maréchal criteria [5] for various wavelengths. Optics that do not reach this quality standard will scatter a substantial amount of radiation. Other requirements of prime importance pertain to slope error, wavefront (WF) distortion, and Strehl ratio. The *Strehl* ratio is the ratio of the maximum intensity at the focus in the presence of WF distortions, divided by the intensity that would be obtained if no distortions were present. The Strehl ratio (SR) depends only on the rms wavefront distortion σ, measured in wavelengths [6].

$$\mathrm{SR} = e^{-(2\cdot\pi\cdot\sigma)^2} \tag{1}$$

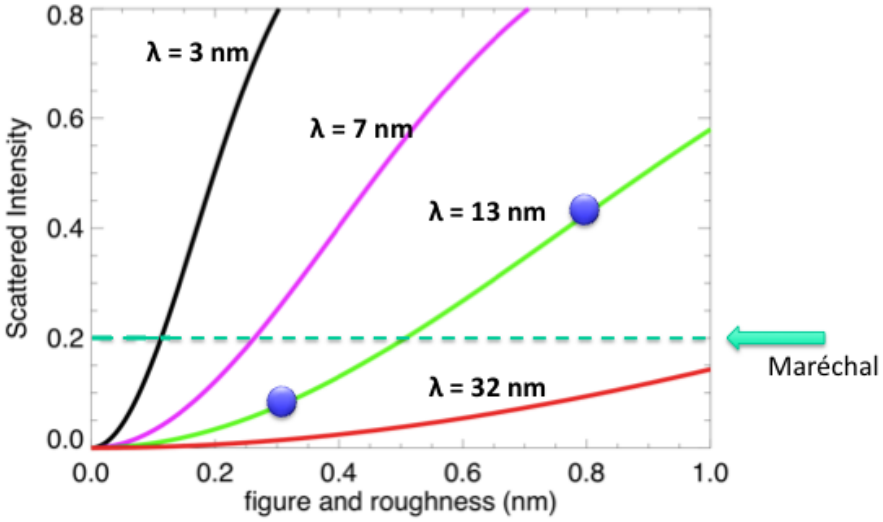

Fig. 1. Scattering intensity versus substrate figure as a function of FEL wavelength for normal incidence geometry.

#114017 - $15.00 USD Received 8 Jul 2009; revised 14 Aug 2009; accepted 1 Sep 2009; published 25 Sep 2009

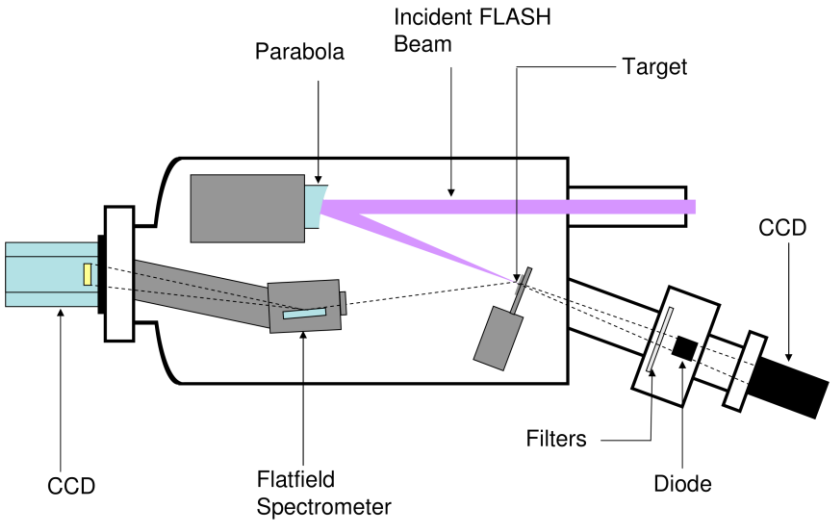

Fig. 2. The 5-mm diameter FLASH beam of 92eV photons is focused with a multi-layer coated off-axis parabola to a focal spot of ~1μm diameter.

WF distortion $\int$ = 1/14 corresponds to Maréchal criterion. The Maréchal criterion states that a system is regarded as well corrected if the Strehl ratio is greater than or equal to 0.8 [5,6]. If these requirements are not met, the highest intensities that the 4th generation sources have to offer will be beyond reach. In addition, better metrology is required for soft X-ray optics that meets the Maréchal criteria for attaining tight focus.

2. Experimental method

The experimental platform at FLASH is shown in schematic form in Fig. 2 and has an angle of 21.8° between the incident and reflected beam. FLASH was operating at a wavelength of 13.5 nm, i.e. photon energy of 92 eV for these experiments. The laser produced pulses of soft X-ray radiation containing between 10 and 50 μJ per pulse in a pulse length of order 15 fs (1) at a repetition rate of 5 Hz. The highly-collimated beam of diameter 5mm was focused onto solid samples using a Mo/Si multilayer (ML)-coated off-axis parabola with a focal length of 270 mm, and an initial reflectivity of 67%. This reflectivity was reduced to 48% after 15 12-hour shifts in the vacuum chamber operating at an average pressure of 1 x 10^{-8} mbar with CH, H_2O, CO and CO_2 present as main contaminants. Under these conditions the mirror developed a dark brownish spot in the center of the optic [7].

Zerodur off-axis paraboloid (OAP) substrates 50 mm in diameter were fine polished by ASML Optics (Richmond, CA) to the surface specification that the first 36 Zernike polynomials should yield 1 nm rms using a proprietary process. Additionally, the RMS surface roughness should be 0.3 nm for both mid spatial frequencies of 1 mm to 1 micron and high spatial frequencies of 1 micron to 50 nm.

The figure test for the OAP optics was a software Null test. The surface was phased using the SASHIMI interferometer at ASML. The resultant data was optimized to compare it against the perfect asphere. In the optimization process, X, Y, and Z-rotation, Z-translation,

#114017 - $15.00 USD Received 8 Jul 2009; revised 14 Aug 2009; accepted 1 Sep 2009; published 25 Sep 2009

and the vertex radius were allowed to float. What this means is that a software algorithm manipulated the data to find the minimal residual error when compared to the perfect shape. Thus, after fine polish, the figure (Z1-Z36) was measured to be 0.3 nm RMS with mid-spatial frequency roughness (MSFR) = 0.148 nm RMS and high spatial frequency roughness (HSFR) = 0.177 nm RMS (Fig. 3a). The combined RMS figure error yields a Strehl ratio of 0.88.

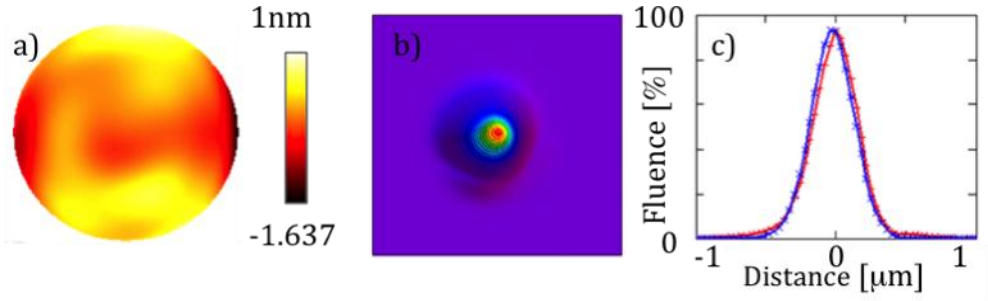

Fig. 3. (a) Measured OAP surface figure error and (b, c) simulated focus. Figure error = 0.3 nm rms. Blue and red lines in the Fig. 3 (c) represent the fluence distribution in the horizontal and the vertical directions respectively. The calculated Strehl ratio is 92.5%.

In order to use the off-axis parabola in normal incidence geometry the substrate was coated with a reflective Mo/Si multilayer coating. The Mo/Si multilayer (ML) coated mirrors were optimized for a wavelength of 13.5 nm and the mirror performance as a function of its angle and wavelengths are reported in detail elsewhere [7] as characterized at the Advanced Light Source B6.3.2 reflectometer [8].

The multilayer-coated optic was mounted in an experimental chamber attached to the end of beamline 3 (BL3) at FLASH, on a custom translatable gimbal stage with x, y, z, theta-x, theta-y and theta-z movements. A preliminary rough alignment of the optic was achieved using He-Ne laser. A long range microscope was used to view craters created by the focused FLASH beam during fine alignment but to get the true beam size ex-situ analyses were performed with Nomarski microscopy and atomic force microscopy (AFM) to measure the size, shape and depth of the crater.

3. Results and discussion

Simulations of the focused beam using the FLASH specifications for the BL3 beamline (Source distance to BL3: 74 m, divergence of the beam: 100μrad FWHM, working distance from optic to focus: ≥ 250 mm) are presented in Fig. 3b. The simulation was performed using the Fourier Optics approach [9]. For large Fresnel numbers, the wavefront propagation (WF) in vacuum was simulated numerically using the Spectral Method (SM) [9]. The Fresnel Integral method (FIM) was used for small Fresnel numbers [9]. This paraxial approximation was justified because the FLASH photon beam was well collimated. Both SM and FIM were implemented into a MATLAB code [10]. The source was assumed to be coherent and a Gaussian beam approximated the FLASH beam with the source size in the beam waist being determined by the divergence of the beam. The Gaussian wavefront was first propagated by the distance between the source and the center of the OAP. Two thin phase shifters modeled the OAP with the first phase shifter corresponding to an ideal lens having the focal length of 250 mm. The second phase shifter accounted for the phase change $\Delta\varphi$ due to the separation of the OAP surface from an ellipsoidal mirror surface. The ellipsoidal mirror had one focus located in the source and the second one in the nominal focus of the OAP. The focal length of the ellipsoidal mirror was also 250 mm. The phase shift $\Delta\varphi$ was determined as follows. First, a line was drawn between a point on the WF grid and the source location S. Then the positions of the intersection points between this line and the OAP surface (point A) and the ellipsoid surface (point A') were calculated. The phase shift resulted from the difference of optical

#114017 - $15.00 USD Received 8 Jul 2009; revised 14 Aug 2009; accepted 1 Sep 2009; published 25 Sep 2009

paths *SAF* and *SA'F*, $\Delta\varphi = 2\pi/\lambda$ *(SAF-SA'F)* where F is the nominal focal point location and λ is the wavelength. After the phase shift operation the WF was propagated a desired distance using SM or FIM algorithms. The simulation shows that the ultimate focused spot diameter is 0.3 μm for this OAP. However, experimental limiting factors affecting the ultimate focus include (1) optic alignment and (2) quality of incoming beam.

Experimental characterization of the focus was accomplished by imprinting the focused single-shot beam profile on a 5 μm PMMA/Si(100) target (ablation threshold for PMMA at 13.5 nm - 25 mJ/cm^2). This technique utilizes the non-thermal, highly localized ablation of the organic polymer providing a smooth surface of the crater interior [2,11,12]. In situ observation of best OAP alignment and focus was accomplished using a long-range microscope to determine focal spot diameter as a function of absolute target position, thus varying the soft X-ray intensity in the regime $10^{13} - 10^{16}$ Wcm^{-2}. After many iterations, ex-situ Nomarski (DIC - differential interference contrast) microscopy (BX51M DIC microscope, Olympus; Japan) and AFM in tapping mode (D3100 NanoScope Dimension controlled by NanoScope IV Control Station, Veeco; USA) were used to characterize the imprinted beam profile and thus focus. The crater shapes, measured by AFM, allow us to reconstruct the beam profile down to the limiting threshold fluence and extract the intensity. Results are presented in Figs. 4a, 4b. These results show that the FWHM of the focus is < 0.7 μm, which confirms that a real micro-focus was achieved with the aligned OAP optic.

Comparisons of the craters' shapes with the results of simulations performed with different wavefront (WF) quality are presented in Fig. 5. In this case, a 3mm diameter circular aperture was placed 22 m downstream of the source. The measurements and the simulations were done at the distance 300 μm with respect to the focal plane based on available imprint data. The observed focal spot (Fig. 5a) is of good quality showing nearly no sign of astigmatism.

The distortions of the craters shape simulated for the WF quality λ/30, λ/15 and λ/10 are presented in Fig. 5b-c for evaluation. The simulated data represent the surface at which the ablation threshold was reached. We applied the same attenuation length and the ablation threshold as used in the beam profile reconstruction procedure (Fig. 4). Clearly, the measured spot exhibits smaller crater rim distortion than the one simulated for WF distortion λ/15 . It follows from the Eq. (1) that the WF distortion λ /15 gives the Strehl ratio equal to 0.84. On other hand, for small WF distortions, the RMS focus size $\boldsymbol{w}$ is inversely proportional to the Strehl ratio: $\boldsymbol{w} = \boldsymbol{w_0}/SR$ where $\boldsymbol{w_0}$ is the diffraction limited ($f = 0$) focal size. In our case $\boldsymbol{w_0}$ = 300 nm FWHM. Results presented in the Fig. 5 indicate that the WF distortions are smaller than λ/15 and that the size of the spot in the focus is smaller than 0.35 μm FWHM.

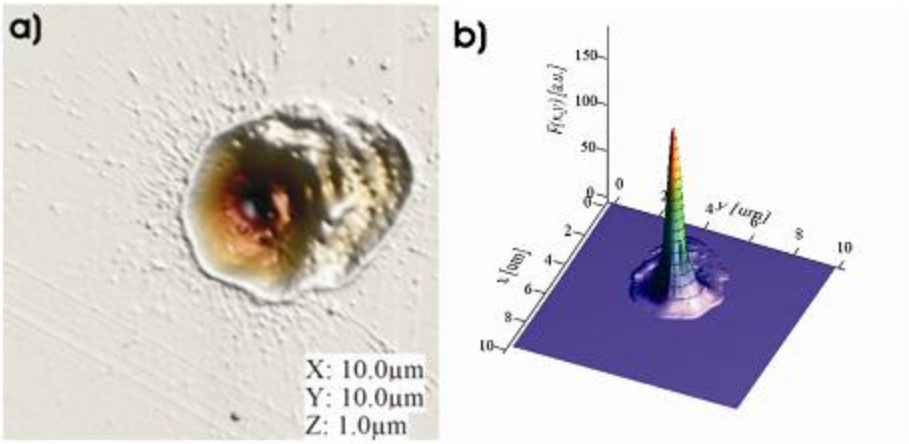

Fig. 4. (a) AFM scan of the crater produced in a PMMA target at tight focus, ≤ 1 μm focus was achieved. (b) Reconstructed beam profile – transverse distribution of relative intensity.

#114017 - $15.00 USD Received 8 Jul 2009; revised 14 Aug 2009; accepted 1 Sep 2009; published 25 Sep 2009

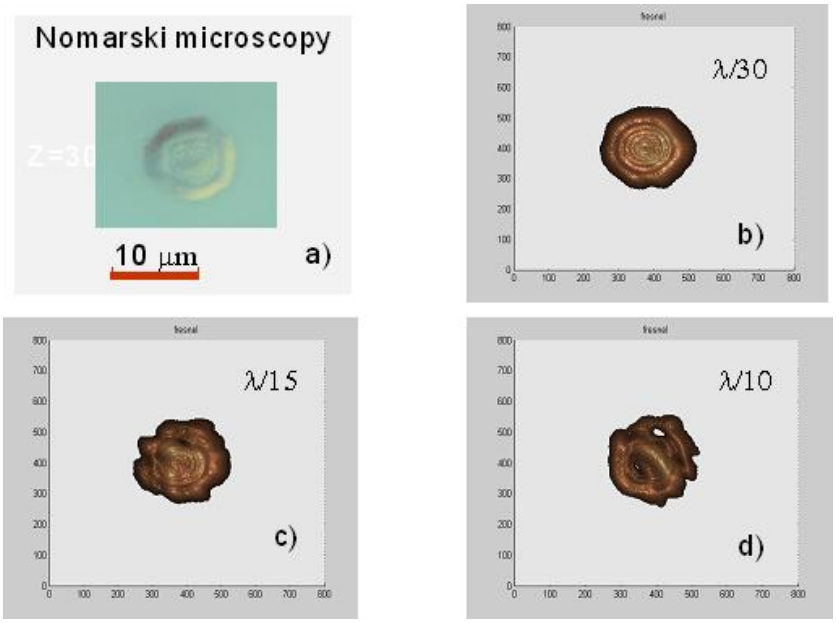

Fig. 5. (a) Nomarski photograph of the spot irradiated in the PMMA sample 300 μm from the focus. (b-c) Simulations of the craters produced by the focused beam having WF quality λ/30 (b), λ/15 (c) and λ/10 (d).

For a comparison, the focusing of the plasma-based soft X-ray laser beams provides irradiances that do not exceed 10^{12} W/cm^2 [13–16]. This intensity limit is strictly given in particular by the focal spot diameter of several tens of micrometers and the pulse duration ranging for the plasma lasers from picosecond [14] to nanosecond [16]. The above-described combination of femtosecond pulses emitted by the free-electron laser and the submicron focal spot size makes it possible to achieve intensities for at least four orders of magnitude higher.

4. Conclusion

We have achieved and characterized a sub-micron focused soft X-ray laser and intensities approaching 10^{17} to 10^{18} W/cm^2. These high intensities were achieved with surface figure specifications for the OAP optical element used in a normal incidence geometry that accounted for slope error, wavefront distortion, and Strehl ratio. Using the Maréchal criteria for good quality optics: Strehl ratio > 0.8 (ratio of the maximum intensity at the focus in the presence of distortions, divided by the intensity that would be obtained if no distortion were present), the corresponding RMS roughness was required to be < 0.5 nm for 13 nm wavelength necessitating improved metrology for this OAP optic to attain the sub-micron tight focus. This focused soft X-ray laser beam and higher intensities has vast implication for further X-ray FEL research and will now allow us to begin exploring matter under extreme conditions. Developing advanced characterization capabilities for probing matter under extreme conditions are important to the emerging field of High Energy Density Science (HEDS).

Acknowledgments

The authors want to acknowledge K. Budil of LLNL for assistance in support in funding and Lou Marchetti at ASML for delivering the OAP with the required specifications. This work was partly performed under the auspices of the U.S. Department of Energy by Lawrence Livermore National Laboratory under Contract DE-AC52-07NA27344. Financial support from Czech Ministry of Education (projects LC510, LC528, and LA08024), Academy of Sciences of the Czech Republic (projects KAN300100702, Z10100523, IAAX00100903, and IAA400100701), and Grant Agency of the Czech Republic (202/08/H057) is greatly

#114017 - $15.00 USD Received 8 Jul 2009; revised 14 Aug 2009; accepted 1 Sep 2009; published 25 Sep 2009

appreciated. Support from the Science and Technology Facilities Council and Engineering and Physical Sciences Research Council is also sincerely appreciated. The Swedish Research Council and the Helmholtz Association (through Virtual Institute VH-VI-302) are acknowledged as well for financial support. We would finally thank the FLASH team at DESY for their continuous support, and we gratefully acknowledge the support for access to FLASH by the European Community under contract RII3-CT-2004-506008 (IA-SFS).

#114017 - $15.00 USD Received 8 Jul 2009; revised 14 Aug 2009; accepted 1 Sep 2009; published 25 Sep 2009